

Diffusion–Controlled Growth of Pearlite in Ternary Steels

BY A. S. PANDIT AND H. K. D. H. BHADESHIA

University of Cambridge
Materials Science and Metallurgy
Pembroke Street, Cambridge CB2 3QZ, U. K.

Abstract

A theory for the diffusion–controlled growth of pearlite in steels containing manganese is presented and assessed in the light of experimental data. Given the overwhelmingly rapid diffusivity that a substitutional solute has within the transformation front, the growth rate is found to be dominated by diffusion parallel to the interface with austenite as the rate controlling step. The relevant interfacial diffusion parameters have been derived by fitting experimental data to kinetic theory. All reported measurements of pearlite growth where the full set of necessary parameters have been listed, are shown to be inconsistent with mechanisms which do not involve the partitioning of substitutional solutes. The method adopted here, which is based on local equilibrium at the transformation interface with the long–range partitioning of substitutional solutes by migration within the interface, has been shown to reasonably explain experimental data over a range of temperatures and chemical compositions.

1. Introduction

In recent work (Pandit and Bhadeshia, 2011), we established a method for calculating the growth rate of pearlite in a binary Fe–C system, without making *a priori* assumptions about whether the process should be controlled by the diffusion of carbon in the bulk of the parent phase, or short–circuited by diffusion in the transformation front, or whether diffusion through the ferrite behind the transformation front plays a role. The method permits all processes to occur simultaneously within an analytical framework with the extent of contribution from particular mechanisms depending naturally on circumstances such as the supercooling below the equilibrium temperature and the pertinent diffusion coefficients. Unlike conventional treatments, no intervention is required in the calculation to see whether the growth rate is, for example, volume or interface diffusion–controlled. This is necessary before the algorithms for pearlite kinetics can be incorporated robustly into schemes for the complete calculation of the major microstructural constituents in steels (Babu et al., 1995; Bhadeshia et al., 1985; Chen et al., 2008; Jones and Bhadeshia, 1997; Umemoto et al., 1987).

The purpose of this paper is to extend this treatment to ternary steels designated Fe–C–X, where ‘X’ stands for a substitutional solute such as manganese. The

complication here is that the diffusivity of a substitutional solute is far smaller than that of interstitial carbon. It then becomes difficult to discover conditions in which all solutes can maintain local equilibrium at the transformation front. The problem was elegantly solved some time ago in the case of the growth of allotriomorphic ferrite from austenite (Coates, 1973; Hillert, 1953; Kirkaldy and Sharma, 1980; Purdy et al., 1964). In essence, there is an additional degree of freedom afforded by the presence of the second solute which permits equilibrium between two phases to exist for a range of compositions, rather than being defined uniquely for a binary alloy. This means that it is possible to pick interface compositions which maintain local equilibrium and yet allow the fluxes of the fast and slow diffusing species to keep pace.

The situation for pearlite is further complicated by the fact that two phases, ferrite and cementite, grow in a coupled manner at a common front with the austenite. It is even possible that local equilibrium, although a well-defined concept, is not in fact maintained during growth. It is relevant therefore to begin with a short assessment of the experimental data that exist on the partitioning of solutes as growth occurs.

(a) *Data on Partitioning of Substitutional Solutes*

Partitioning describes the redistribution of solute between the phases participating in the transformation process. Early studies in the context of pearlite in Fe–C–Mn and Fe–C–Cr indicated a so-called no-partition temperature below which the substitutional solute does not redistribute and pearlite growth is limited by the diffusion of carbon (Razik et al., 1974, 1976). It was argued that above this temperature, it is the diffusion of X through the transformation interface that determined the growth rate. However, neither of these scenarios was able to correctly estimate the growth rate at low temperatures.

Al-Salman et al. (1979) found that both chromium and manganese partitioned into cementite at the growth front in a Fe–Cr–Mn–C alloy down to a transformation temperature of 600°C, but were unable to identify a no-partition temperature. Experiments conducted with better resolution on Fe–Cr–C revealed that chromium in fact continues to partition in this manner to temperatures as low as 550°C (Chance and Ridley, 1981), with the extent of partitioning increasing with temperature; once again, a no-partitioning temperature could not be identified. It was demonstrated that the rate of growth at low temperatures could be explained equally well by carbon volume diffusion or interfacial diffusion of chromium; there is of course, no logical reason to assume that the flux of carbon should be confined to the volume without a contribution through the interface. Hutchinson *et al.* studied the partitioning behaviour of steels containing 3.5 wt% Mn and observed that it partitioned significantly during transformation at 625°C, but the measurements were on samples heat treated for 2.5 h in which case it is not established whether the redistribution of solute occurred during growth or as a consequence of the extended heat treatment following the cessation of growth.

The experimental observations to date can lead to one firm conclusion, that substitutional solutes do partition at all temperatures where pearlite is known to grow; this might be expected since the transformation is reconstructive. It may reasonably be assumed that when a temperature is reached where the mobilities

of the substitutional atoms are sufficiently small, pearlite simply ceases to form and austenite transforms instead by a displacive mechanism. We now proceed to develop and assess the growth process for pearlite in ternary steels.

2. Local Equilibrium in Ternary Systems

One well-known difficulty in dealing with ternary steels is that the interstitial carbon typically diffuses many orders of magnitude faster than substitutional solutes. To maintain local equilibrium at the interface, the rate at which solute is absorbed (or rejected) by the growing phase must equal that at which it arrives by diffusion (or diffuses away) from at the interface. This requires the following two equations, one for each solute, to be satisfied simultaneously,

$$(c_C^{\gamma\alpha} - c_C^{\gamma\theta})v = -D_C \nabla c_C \quad (2.1)$$

$$(c_{Mn}^{\gamma\alpha} - c_{Mn}^{\gamma\theta})v = -D_{Mn} \nabla c_{Mn} \quad (2.2)$$

where the symbols α , γ and θ stand for ferrite, austenite and cementite respectively, v is the velocity of the transformation front and $c_C^{\gamma\alpha}$ is the concentration of carbon in the austenite which is in equilibrium with ferrite; the other concentration terms are similarly interpreted and D represents the diffusivity of the solute identified by the subscript. Given that $D_C \gg D_{Mn}$, there are two ways of choosing a tie-line which can satisfy these equations (Coates, 1972, 1973), involving either the maximisation of ∇c_{Mn} or the minimisation of ∇c_C ; in the former case the sluggish diffusion of Mn is compensated for by selecting a tie-line which maximises its gradient, and in the latter case the tie-line is such that the gradient of carbon is minimised, thus allowing the two solutes to keep pace with the single moving interface.

For simplicity, we first illustrate these scenarios for the growth of a single phase, ferrite, from austenite; as will be seen later, even this simple presentation can clarify the mechanism of pearlite growth. The case where the gradient of carbon is diminished is illustrated in Fig. 1a, where the austenite is supercooled into the two-phase field near the $\alpha + \gamma/\gamma$ boundary. This necessitates the partitioning and hence long range diffusion of manganese so the mode is designated ‘partitioning local equilibrium’ (P-LE). In contrast, a large supersaturation, whence the austenite is supercooled to a location in the two-phase field close to the $\alpha + \gamma/\alpha$ boundary leads to the case where the Mn concentration in α is similar to that in the alloy, or the ‘negligible partitioning local equilibrium’ (NP-LE) mode (Fig. 1b). Note that both cases involve local equilibrium at the interface and are exclusive; Fig. 1c shows the domains of the two-phase field within which each of the modes operates. A simple examination of the location of the alloy within the $\alpha + \gamma$ phase field therefore can establish whether or not Mn will partition during *ferrite growth* or whether growth will occur with negligible partitioning of the substitutional solute. The important point to recognise is that if partitioning must occur during ferrite growth then it necessarily means that pearlite growth must also involve partitioning since the ferrite is one component of pearlite.

This discussion of the growth of ferrite is well-established (Coates, 1972, 1973) but it can be applied immediately to reach conclusions about pearlite, where two phases grow from austenite. It is necessary then to consider both the $\alpha + \gamma$ and $\theta + \gamma$ phase fields, and two separate tie-lines must be chosen to fix the compositions

at the α/γ and θ/γ interfaces, as illustrated in Fig. 1d. The case illustrated is for NP-LE and it is only possible for the alloy marked ‘A’ to transform in this manner because the situation illustrated corresponds to a high-supersaturation meaning thereby that the alloy is far from the $\gamma/\gamma + \alpha$ boundary. We find that growth with NP-LE is thermodynamically not possible for any of the experimental data (Razik et al., 1974, 1976) reported for the growth of pearlite.

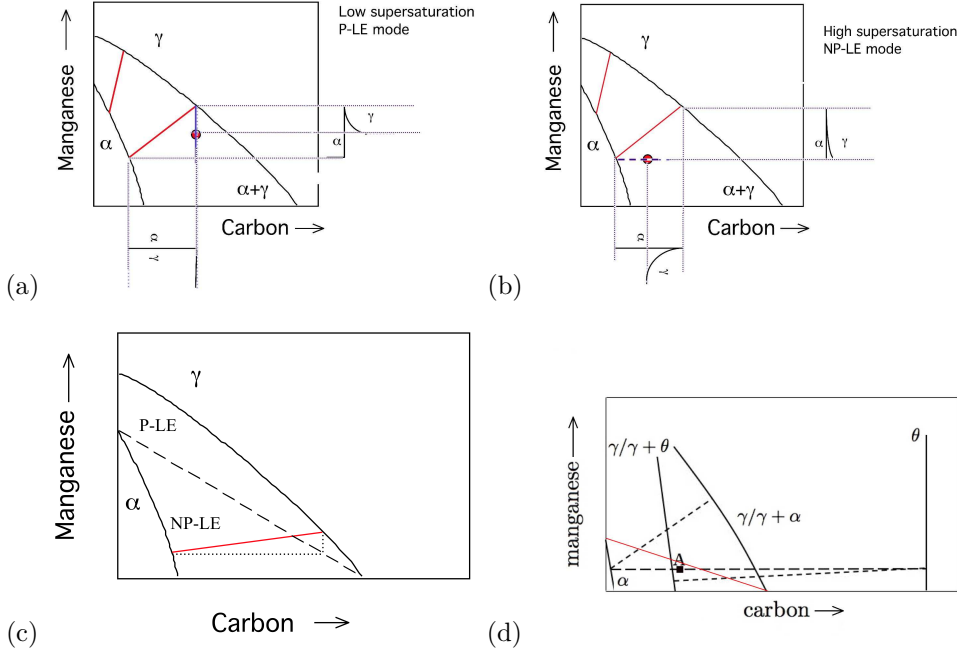


Figure 1. (a–c) Growth of ferrite with local equilibrium at the interface. The tie-lines are illustrated in red. When the alloy (indicated by dot) in its austenitic state is quenched into the $\alpha + \gamma$ phase field, the supersaturation is small if the alloy falls close to the $\alpha + \gamma/\gamma$ phase boundary. (a) P-LE mode involving the long-range diffusion of manganese. (b) NP-LE mode with negligible partitioning of Mn. (c) Division of the two-phase $\alpha + \gamma$ phase field into NP-LE and P-LE domains. For more details see (Bhadeshia, 1985). (d) Schematic ternary isothermal section for the NP-LE condition satisfied for both cementite and ferrite during the growth of pearlite. The composition marked ‘A’ falls in the NP-LE region where the red line separates the NP-LE and P-LE domains for ferrite.

The partitioning local-equilibrium case corresponds to one in which the activity of carbon in the austenite ahead of the interface is almost uniform, thus allowing the flux of the slow diffusing manganese to keep pace. The activity of carbon in austenite for the alloy composition was calculated using MTDATA. The point of intersection of the carbon iso-activity line with the phase boundaries of $\gamma/\gamma + \theta$ and $\gamma/\gamma + \alpha$ gives the interfacial compositions of Mn in austenite in equilibrium with ferrite and cementite. The tie-line corresponding to these points should then give the quantities $c_{Mn}^{\alpha\gamma}$, $c_{Mn}^{\gamma\alpha}$, $c_{Mn}^{\theta\gamma}$ and $c_{Mn}^{\gamma\theta}$.

It is found that the iso-activity line passing through the point Fe-0.8C-1.0Mn wt % never intersects the $\gamma/\gamma + \theta$ phase boundary, as has been observed in previous

work for a series of Fe–Mn–C hypo–eutectoid steels (Hutchinson et al., 2004). The strict P–LE condition is therefore impossible to achieve. The best that can be done in order to set $c_{\text{Mn}}^{\gamma\theta}$ whilst at the same time ensuring that $c_{\text{Mn}}^{\gamma\theta} < \bar{c}_{\text{Mn}} < c_{\text{Mn}}^{\theta\gamma}$, where \bar{c} is the average composition of the alloy, is to assume that the tie-line connecting cementite and austenite passes through the alloy composition as illustrated for 945 K in Fig. 2.

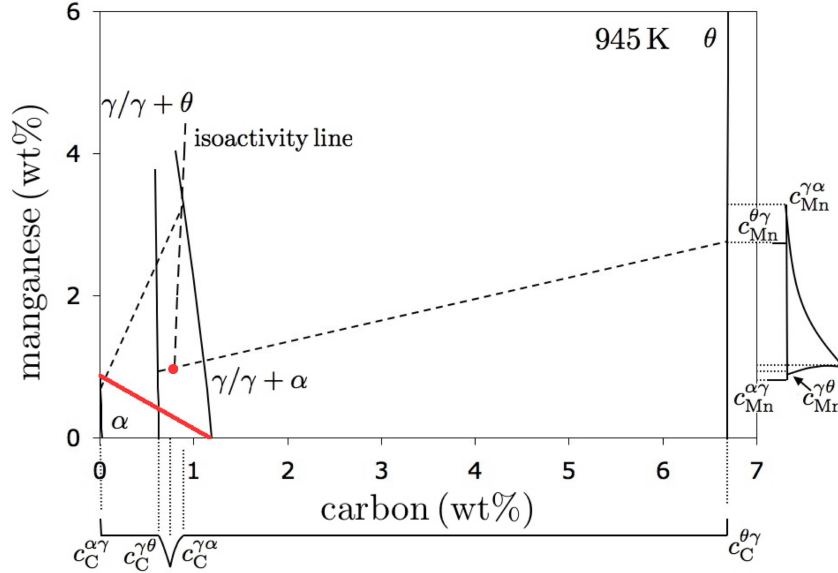


Figure 2. The case for partitioning local equilibrium transformation of Fe–0.8C–1Mn wt%, noting that strict P–LE is not possible since the carbon iso–activity line does not intersect the $\gamma + \theta/\gamma$ phase boundary. The alloy is indicated by the red dot and the red line divides the $\alpha + \gamma$ phase fields into the P–LE and NP–LE domains.

3. Pearlite Growth Rate in Fe–Mn–C Steels

(a) Assumptions

It is assumed that the transfer of atoms across the growth front is not rate limiting; for a diffusion–controlled reaction, the compositions at the interfaces can be estimated from the existence of local equilibrium. In such a case, the compositions are given by tie–lines of the equilibrium ternary phase diagram so that the chemical potentials (μ) of the species are locally uniform:

$$\begin{aligned} \mu_{\text{Fe}}^{\gamma} &= \mu_{\text{Fe}}^{\alpha} & \text{and } \mu_{\text{C}}^{\gamma} &= \mu_{\text{C}}^{\alpha} & \text{and } \mu_{\text{Mn}}^{\gamma} &= \mu_{\text{Mn}}^{\alpha} \\ \mu_{\text{Fe}}^{\gamma} &= \mu_{\text{Fe}}^{\theta} & \text{and } \mu_{\text{C}}^{\gamma} &= \mu_{\text{C}}^{\theta} & \text{and } \mu_{\text{Mn}}^{\gamma} &= \mu_{\text{Mn}}^{\theta} \end{aligned}$$

Since the kinetic theory for pearlite gives the growth rate as a function of interlamellar spacing rather than a unique velocity, it is assumed that the actual

spacing adopted is the one which leads to maximisation of the entropy production rate (Kirkaldy and Sharma, 1980).

The preceding discussion based on experimental observations indicates that substitutional solutes partition during the growth of pearlite even at the lowest of temperatures studied. Furthermore, none of the data are consistent with growth involving local equilibrium with negligible partitioning. In addition, only an approximation to the P–LE mode can apply if local equilibrium is to be maintained, since the iso-activity line for carbon does not in general intersect the $\gamma/\gamma+\theta$ phase boundary; it is necessary, therefore, to assume that the tie-line connecting cementite and austenite passes through the alloy composition.

We now proceed to calculate the growth rates based on this set of assumptions, bearing in mind that substitutional solutes must diffuse, and that the easiest diffusion path for such solutes is through the interface. We have verified by calculation that the substitutional solute flux through the volume of the austenite is negligibly small by comparison.

(b) *Activation energy for boundary diffusion*

Whereas data for volume diffusion are readily available, those for boundary diffusion are not. Use was therefore made of experimental data on pearlite growth where interlamellar spacings have also been measured and reported. Such data are available for 1.0 wt% (Ridley, 1984) and 1.08–1.8 wt% Mn eutectoid steels (Razik et al., 1974). The data from (Ridley, 1984) were used to derive interfacial diffusion coefficients by fitting to the theory for boundary diffusion-controlled growth of pearlite (Hillert, 1957):

$$v = 12kD_B \delta \left(\frac{c_{Mn}^{\gamma\alpha} - c_{Mn}^{\gamma\theta}}{c_{Mn}^{\theta\gamma} - c_{Mn}^{\alpha\gamma}} \right) \frac{1}{S^\alpha S^\theta} \left(1 - \frac{S_c}{S} \right) \quad (3.1)$$

where v is the growth rate of pearlite, k is the boundary segregation coefficient for the γ/α and γ/θ interfaces, the values of which are difficult to determine experimentally and hence are not available. The thickness of the transformation interface, δ , is assumed to be of the order of 2.5 Å. S^α and S^θ are the thicknesses of the ferrite and cementite platelets. In order to avoid any assumptions regarding the segregation coefficient, a lumped value of kD_B is evaluated from the experimental data of Ridley (Ridley, 1984). The critical interlamellar spacing S_c at which $v = 0$ was calculated from $S/S_c = 2$ based on the growth rate which leads to the maximum rate of entropy production (Kirkaldy and Sharma, 1980; Pandit and Bhadeshia, 2011). Phase equilibria were, throughout this work, calculated using MTDATA and the TCFE database (NPL, 2006). Fig. 3 shows a plot of $\ln kD_B$ vs. $1000/T$, the slope and intercept of which yields the boundary diffusion coefficient for manganese:

$$kD_B = 2.81 \times 10^{-3} \exp \left(-\frac{164434 \text{ J mol}^{-1}}{RT} \right) \text{ m}^2 \text{ s}^{-1} \quad (3.2)$$

(c) *Interfacial energy*

The interfacial energy per unit area σ for the ferrite-cementite interface can also be derived from the kinetic data available for pearlite growth. The critical spacing

at which growth ceases because all of the driving force is used up in creating the interfaces is given by:

$$\sigma = \frac{1}{2} S_c \Delta G \approx \frac{S_c \Delta T \Delta H}{2T_E} \quad (3.3)$$

The approximation on the extreme right hand side is based on the assumption that the entropy of transformation is independent of temperature (Capdevila et al., 2002; Offerman et al., 2003; Ridley, 1984). This can be overcome by calculating the enthalpy and entropy changes using MTDATA (NPL, 2006) and the same has been shown in Fig. 4. The critical spacing S_c is calculated from the experimentally measured interlamellar spacings S (Ridley, 1984) and the graphical relation of S/S_c shown in Fig. 5. The ratio S/S_c is calculated assuming the maximum entropy production rate and is equal to 2 for the range of temperatures studied; this is unlike the previous study on Fe-C alloy (Pandit and Bhadeshia, 2011), simply because with the substitutional solute it is only the flux through the interface which is relevant, whereas in the case of carbon, the proportions contributed by volume and interface diffusion vary significantly with temperature. The interfacial energy estimated in this way is shown in Fig. 6. For reasons which are not clear, the values thus calculated are somewhat higher than those reported for Fe-C but not dramatically different.

It is important to note that in all of the analysis of experimental data (v, S) that follows, the interfacial energy does not appear explicitly since equation 3.1 requires only the ratio S_c/S . Given measured values of S and the fact that $S/S_c = 2$ means that S_c is defined. However, in order to make *predictions* of the growth rate in the absence of experimental data, it clearly is necessary to know the interfacial energy.

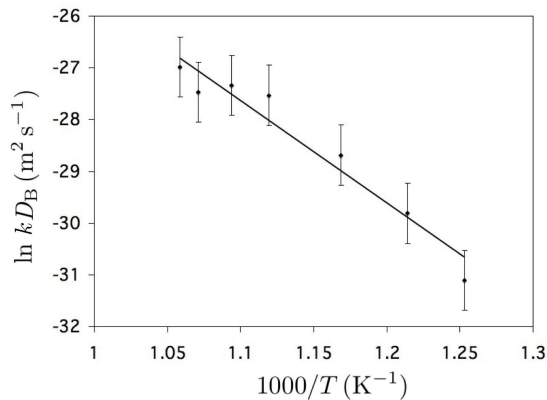


Figure 3. Arrhenius plot of D_B versus inverse of temperature in Fe-1.0Mn-0.8C wt% steel for interface diffusion controlled pearlite growth.

(d) Calculation of Growth rate

The pearlite growth rate calculated assuming partitioning local equilibrium (PLE) is shown in Fig. 7. There is a reasonably good match with the measured growth rate for 1.0 wt% Mn steel (Ridley, 1984); that in itself is not surprising since the boundary diffusion coefficients and interfacial energies were derived using those data. The pearlite growth rate was also calculated for a steel containing 1.8

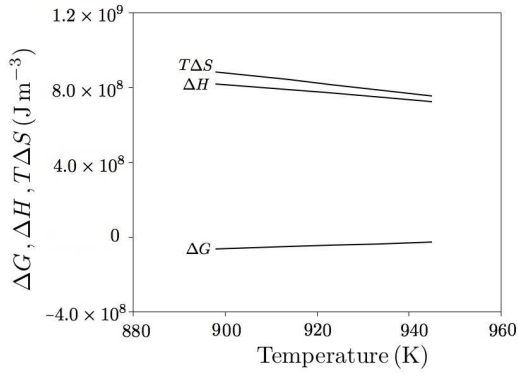


Figure 4. Free energy, enthalpy and entropy change as a function of temperature.

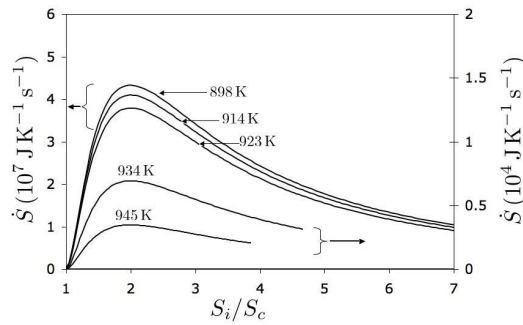


Figure 5. Variation in the entropy production rate as a function of the interlamellar spacing.

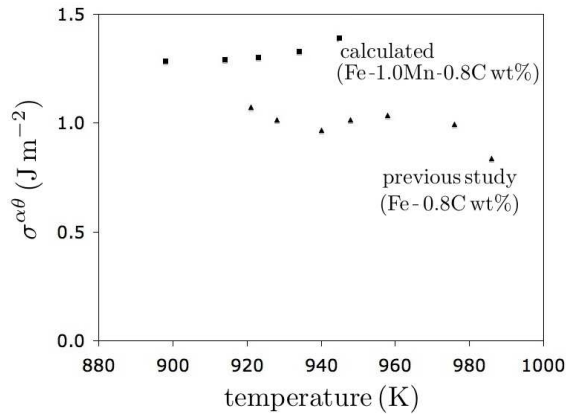


Figure 6. Ferrite-cementite interfacial energy compared with those from previous study for Fe-C steels (Pandit and Bhadeshia, 2011).

wt% Mn and there seems to be a good fit with the experimental growth rate determined by Razik et al. (1974) at low temperatures, although at higher temperatures the difference increases.

In order to extend the applicability of the theory discussed in this paper for steels containing Mn, the pearlite growth rate was calculated for Fe-1.29Cr-0.82C wt% based on the work of Razik et al. (1976). There is one complication when the data corresponding to 993 and 1003 K are considered. Because the alloy has a

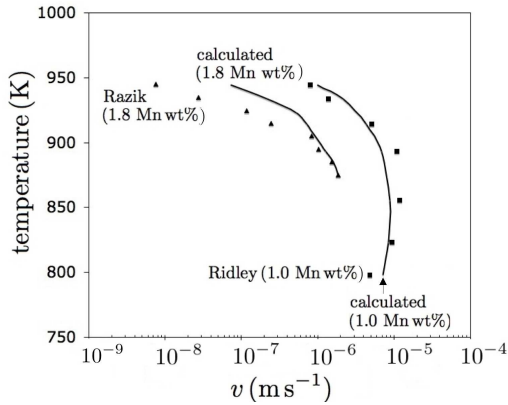


Figure 7. Pearlite growth rate as a function of temperature for Fe-1.0Mn-0.8C wt% and Fe-1.8Mn-0.69C wt%. Solid lines are calculated.

carbon concentration which is hypereutectoid, the supercoolings at these particular transformation temperatures are not sufficient to permit ferrite to form until the carbon concentration of the austenite is reduced by the precipitation of cementite. Since both ferrite and cementite must be able to grow from austenite in order to form pearlite, it is assumed that this condition is satisfied when the austenite composition is reduced by the precipitation of cementite to the point where the $\alpha + \gamma/\gamma$ and $\theta + \gamma/\gamma$ phase boundaries intersect, as illustrated by the point 'A' in Fig. 8.

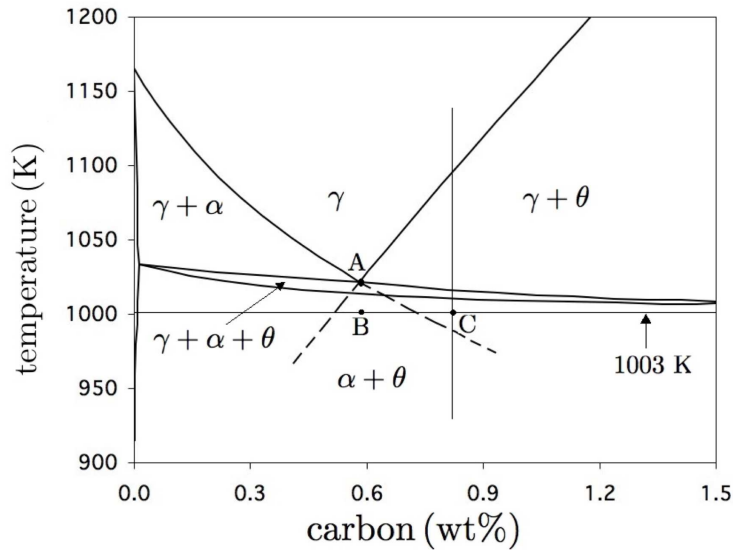


Figure 8. The point 'A', which extrapolates to 'B' at the transformation temperature, is the composition of austenite assumed to decompose into pearlite when the supercooling is insufficient for the hypereutectoid alloy to permit the simultaneous precipitation. The average composition of the alloy is marked 'C' and has a carbon concentration which falls to the right of the extrapolated $\gamma + \alpha/\gamma$ phase boundary, making it impossible to simultaneously precipitate ferrite and cementite.

The interfacial energy has been determined for the steel containing Cr and it lies in the range of 0.52-0.89 J m^{-2} for the temperature range of 1003-933 K (Fig. 9). The lower values of $\sigma^{\alpha\theta}$ obtained can be explained by the greater tendency of Cr to segregate.

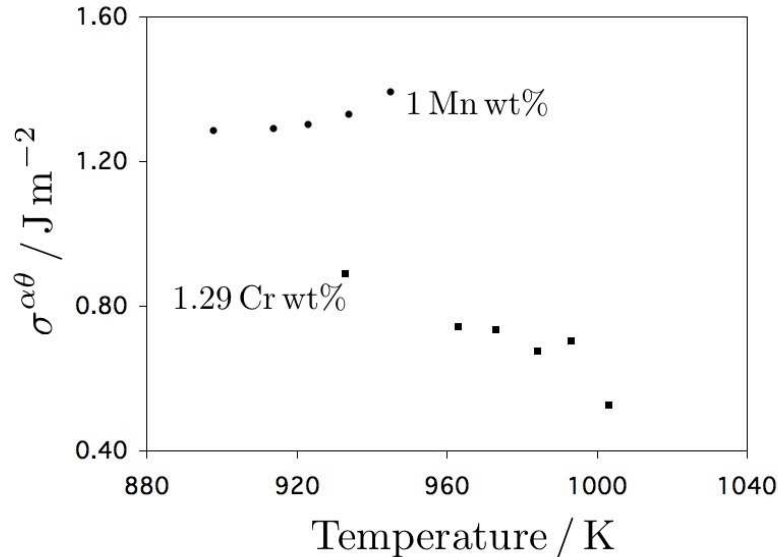


Figure 9. Comparison of ferrite-cementite interfacial energy for Fe-C-Cr and Fe-C-Mn steels.

We have verified that none of the reported data are consistent with the negligible partitioning local equilibrium mode; all of the experiments involve transformation at low supersaturations so that the analysis again is based on partitioning local equilibrium. The boundary diffusivity of chromium, is, in the absence of data, assumed to be identical that of manganese; this is considered to be a good approximation (Fridberg et al., 1969). It is observed that the growth rate estimated assuming the partitioning local equilibrium theory match measured values rather well as shown in Fig. 10. Razik et al. (1976) in assessing their experimental data also calculated growth rates but not for the exact composition of the material studied, rather for an Fe-0.7C-1Cr wt% steel. Their calculations assume that chromium does not partition at all below the dashed horizontal line, so that pearlite growth is controlled by carbon diffusion alone. It is evident that such an analysis either greatly overestimates the growth rate when carbon is taken to diffuse through the interface, and under-predicts when carbon is taken to diffuse through the volume of the austenite ahead of the transformation front.

For both the 1.8 Mn (Fig. 7) and 1.29 Cr (Fig. 10) alloys, the calculated growth rates at the highest of transformation temperatures is greater than those measured. It is possible in ternary steels for the transformation at high temperatures to occur where the three-phases $\gamma+\alpha+\theta$ exist in equilibrium, which would require the volume diffusion of substitutional solutes as the composition of the austenite changes during

the course of transformation. This would result in a reduction in growth rate and an increase in interlamellar spacing (Cahn and Hagel, 1963; Fridberg and Hillert, 1970). However, this is not the explanation for the observed discrepancy since in all cases the reported transformations occur in a phase field where only $\alpha + \theta$ are ultimately in equilibrium. The reasons for the discrepancy are therefore not clear.

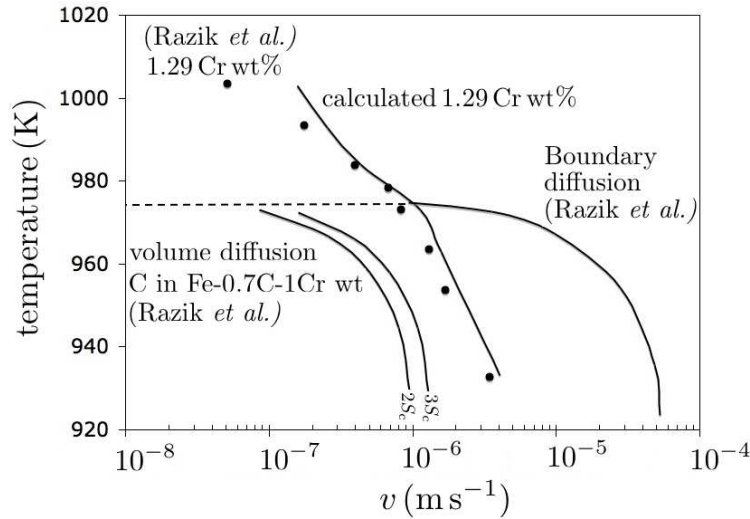


Figure 10. Comparison of calculated and experimental pearlite growth rate as a function of temperature for Fe-1.29Cr-0.82C wt%. The original calculations from (Razik et al., 1976) are included for comparison; the two values of $S/S_c = 2, 3$ for volume diffusion controlled growth correspond to the maximum growth rate and maximum entropy production criteria respectively. The dashed line represents their no-partition temperature.

4. Predictions

Assuming that partitioning local equilibrium governs the conditions at the transformation front, that the interfacial diffusivity derived here is generally applicable, and that the maximum entropy production principle applies, the significant uncertainty in making predictions of the growth rate lies in the value of interfacial energy that must be used to determine interlamellar spacings. The extent of uncertainty may be assessed by using the maximum and minimum values determined from the Fe-1Mn-0.8C wt% system where the range is 1.28–1.39 J m^{-2} with a mean value of 1.32 J m^{-2} . Fig. 11 illustrates the difference these limits make to the growth rate of pearlite. It is suggested that in the absence of reliable data, it may be appropriate to use the mean value reported here accompanied by an error bar which is based on the range of $\sigma^{\alpha\theta}$.

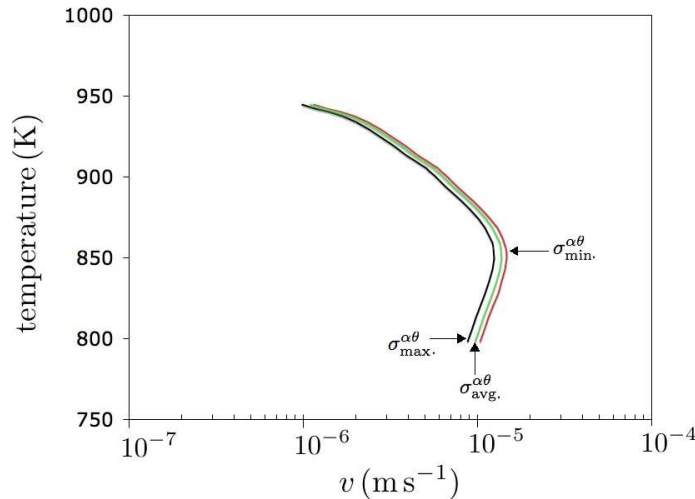


Figure 11. Sensitivity of the growth rate calculations to the α/θ interfacial energy.

5. Conclusions

It has been demonstrated that in circumstances where an analytical calculation of the growth rate of pearlite in ternary steels is useful, all of the published data are inconsistent with transformation in which the solute does not partition between the phases during transformation. Furthermore, even when partitioning is considered, none of the experimental data fall into the category of ‘negligible-partitioning local equilibrium’. If local equilibrium is to be maintained then there is only one option possible, that in which the substitutional solute must diffuse over distances comparable with the interlamellar scale of the pearlite structure. Since the diffusivity of substitutional solutes is much lower than that of carbon, the flux along the interface is by far the dominant mechanism for redistribution of atoms such as manganese or chromium. The experimental data can reasonably be calculated on this basis for steels containing manganese or chromium as ternary additions, and it is possible that the results can be extrapolated to other such substitutional solutes if pragmatic assumptions regarding interfacial energy and diffusivity are justified.

The method adopted here is capable of providing reasonable estimates of pearlite growth using an analytical equation due to Hillert, in combination with thermodynamic data and the assumption that the interlamellar spacing adopted is consistent with the maximum entropy production rate.

A number of difficulties have also been identified, for example, the fact that with hypereutectoid alloys there are circumstances when the simultaneous precipitation of ferrite and cementite is not possible when transforming at low supersaturations, so that it becomes necessary to allow the precipitation of cementite alone prior to the onset of pearlite. The growth rate is dependent on the α/θ interfacial energy and it is currently necessary when making predictions to assume approximate values derived from specific alloy systems; the dependence of interfacial energy on the

chemical compositions at the transformation front is a rich and difficult area for future research.

Acknowledgments

The authors value the considerable support of TATA Steel towards this work, and are grateful to Professor Lindsay Greer for the provision of laboratory facilities at the University of Cambridge.

References

- Al-Salman, S. A., Lorimer, G. W., Ridley, N., 1979. Pearlite growth kinetics and partitioning in a cr-mn eutectoid steel. *Metallurgical Transactions A* 10A, 1703–1709.
- Babu, S. S., David, S. A., Vitek, J. M., Mundra, K., DebRoy, T., 1995. Development of macro- and microstructures of C-Mn low alloy steel welds – inclusion formation. *Materials Science and Technology* 11, 186–199.
- Bhadeshia, H. K. D. H., 1985. Diffusional formation of ferrite in iron and its alloys. *Progress in Materials Science* 29, 321–386.
- Bhadeshia, H. K. D. H., Svensson, L.-E., Gretoft, B., 1985. Model for the development of microstructure in low alloy steel (Fe-Mn-Si-C) weld deposits. *Acta Metallurgica* 33, 1271–1283.
- Cahn, J. W., Hagel, W. C., 1963. Divergent pearlite in a manganese eutectoid steel. *Acta Metallurgica* 11, 561–574.
- Capdevila, C., Caballero, F. G., de Andres, C. G., 2002. Kinetics model of isothermal pearlite formation in a 0.4C-1.6Mn steel. *Acta Materialia* 50, 4629–4641.
- Chance, J., Ridley, N., 1981. Chromium partitioning during isothermal transformation of a eutectoid steel. *Metallurgical Transactions A* 12A, 1205–1213.
- Chen, J., Bhadeshia, H. K. D. H., Hasler, S., Roelofs, H., Ulrau, U., 2008. Complete calculation of steel microstructure for strong alloys. In: Pérez, T. (Ed.), *New Developments on Metallurgy and Applications of High Strength Steels*, Buenos Aires. Vol. 2. TMS-AIME, Materials Park, Ohio, USA, pp. 749–759.
- Coates, D. E., 1972. Diffusion controlled precipitate growth in ternary systems i. *Metallurgical Transactions* 3, 1203–1212.
- Coates, D. E., 1973. Diffusional growth limitation and hardenability. *Metallurgical Transactions* 4, 2313–2325.
- Fridberg, J., Hillert, M., 1970. Ortho-pearlite in silicon steels. *Acta Metallurgica* 18, 1253–1260.
- Fridberg, J., Torndahl, L.-E., Hillert, M., 1969. Diffusion in iron. *Jernkontorets Annaler* 153, 263–276.

- Hashiguchi, K., Kirkaldy, J. S., 1984. Pearlite growth by combined volume and phase boundary diffusion. *Scandinavian Journal of Metallurgy* 13, 240–248.
- Hillert, M., 1953. *Paraequilibrium*. Tech. rep., Swedish Institute for Metals Research, Stockholm, Sweden.
- Hillert, M., 1957. Role of interfacial energy during solid–state phase transformations. *Jernkontorets Annaler* 141, 757–789.
- Hutchinson, C. R., Hackenberg, R. E., Shiflet, G. J., 2004. The growth of partitioned pearlite in Fe–C–Mn steels. *Acta Materialia* 52, 3565–3585.
- Jones, S., Bhadeshia, H. K. D. H., 1997. Kinetics of the simultaneous decomposition of austenite into several transformation products. *Acta Materialia* 45, 2911–2920.
- Kirkaldy, J. S., Sharma, R. C., 1980. Stability principles for lamellar eutectoid(ic) reactions. *Acta Metallurgica* 28, 1009–1021.
- NPL, 2006. MTDATA. Software, National Physical Laboratory, Teddington, U.K.
- Offerman, S. E., van Wilderen, L. J. G. W., van Dijk, N. H., Sietsma, J., th.Rekvelde, M., van der Zwaag, S., 2003. In situ study of pearlite nucleation and growth during isothermal austenite decomposition in nearly eutectoid steel. *Acta Materialia* 51, 3927–3938.
- Pandit, A. S., Bhadeshia, H. K. D. H., 2011. Mixed diffusion-controlled growth of pearlite in binary steel. *Proceedings of the Royal Society A* 467, 508–521.
- Purdy, G. R., Weichert, D. H., Kirkaldy, J. S., 1964. The growth of proeutectoid ferrite in ternary Fe–C–Mn austenites. *Trans. TMS-AIME* 230, 1025–1034.
- Razik, N. A., Lorimer, G. W., Ridley, N., 1974. An investigation of manganese partitioning during the austenite–pearlite transformation using analytical electron microscopy. *Acta Metallurgica* 22, 1249–1258.
- Razik, N. A., Lorimer, G. W., Ridley, N., 1976. Chromium partitioning during the austenite–pearlite transformation. *Metallurgical Transactions A* 7A, 209–214.
- Ridley, N., 1984. The pearlite reaction. In: Marder, A. R., Goldstein, J. I. (Eds.), *Phase Transformations in Ferrous Alloys*. TMS–AIME, Warrendale, Pennsylvania, USA, pp. 201–236.
- Umemoto, M., Guo, Z. H., Tamura, I., 1987. Effect of cooling rate on grain size of ferrite in a carbon steel. *Materials Science and Technology* 3, 249–255.

**Proceedings of the Royal Society of London – A
467 (2011) 2948–2961.**